



RESEARCH ARTICLE

# *In silico* phylogenetic analysis reveals nuclear ribosomal DNA as the most effective marker for DNA barcoding of *Cucumis* L. species

Bagus Herwibawa<sup>1\*</sup>, Florentina Kusmiyati<sup>1</sup>, Muhamad Ghazi Agam Sas<sup>1</sup>, Albertus Fajar Irawan<sup>1</sup>, Siti Novridha Andini<sup>2</sup> & Triono Bagus Saputro<sup>3</sup>

<sup>1</sup>Department of Agroecotechnology, Faculty of Animal and Agricultural Sciences, Universitas Diponegoro, Semarang 50275, Indonesia

<sup>2</sup>Department of Food Crop Production, Politeknik Negeri Lampung, Rajabasa Bandar Lampung 35141, Indonesia

<sup>3</sup>Department of Biology, Faculty of Sciences and Data Analytics, Institut Teknologi Sepuluh Nopember, Surabaya 60115, Indonesia

\*Correspondence email - [bagus.herwibawa@live.undip.ac.id](mailto:bagus.herwibawa@live.undip.ac.id)

Received: 12 January 2025; Accepted: 21 April 2025; Available online: Version 1.0: 14 July 2025; Version 2.0: 24 July 2025

**Cite this article:** Herwibawa B, Kusmiyati F, Sas MGA, Irawan AF, Andini SN, Saputro TB. *In silico* phylogenetic analysis reveals nuclear ribosomal DNA as the most effective marker for DNA barcoding of *Cucumis* L. species. Plant Science Today. 2025; 12(3): 1-13. <https://doi.org/10.14719/pst.6289>

## Abstract

*Cucumis* L. species represent a globally important crop genus with high economic value and genetic diversity, yet their wild relatives remain understudied and potentially threatened by habitat loss and genetic erosion. This knowledge gap hinders effective conservation strategies and limits the utilization of wild genetic resources for crop improvement. A deeper understanding of *Cucumis* diversity and evolution is especially critical for conserving wild relatives of cultivated species, which may harbor valuable traits for climate resilience and disease resistance. This study investigated the effectiveness of 3 DNA barcode markers (*matK*, *rbcl* and *nrDNA*) for phylogenetic analysis across 38 *Cucumis* species, addressing a key methodological gap in Cucurbitaceae systematics with direct applications in germplasm conservation and crop improvement programmes. Sequences were retrieved from NCBI and analyzed using MEGA 11, DnaSP v6 and PopArt. The hypothesis that nuclear ribosomal DNA (*nrDNA*) would outperform plastid markers (*matK* and then *rbcl*) in resolving species relationships was validated. The *nrDNA* displayed the highest genetic distance and clearest clade separation of intraspecific variation, making it particularly valuable for: (i) accurate identification of wild *Cucumis* germplasm in conservation efforts, (ii) precise selection of genetic resources for breeding programmes and (iii) resolution of taxonomic uncertainties in agricultural and ecological studies. *matK* provided moderate resolution, while *rbcl* performed poorly at the intraspecific level. These findings provide a robust molecular toolkit for biodiversity conservation and sustainable agricultural development, enabling more effective utilization and protection of *Cucumis* genetic resources worldwide.

**Keywords:** haplotype network; snp markers; species identification

## Introduction

The genus *Cucumis* L. exhibits remarkable diversity among its cultivated varieties, with cantaloupe melons representing the most widely cultivated type (1). As a diploid plant species (with 2 sets of chromosomes denoted as  $2n = 2x = 24$ ), *Cucumis* belongs to the Cucurbitaceae family, which comprises approximately 965 species of flowering plants (2). The genus includes about 33 recognized species, encompassing both economically important crops such as *Cucumis melo* (melon), *Cucumis sativus* (cucumber) and *Cucumis metuliferus* (horned melon), as well as wild relatives (3). These species are predominantly distributed across tropical and subtropical regions, where they are typically herbaceous and angular, trailing or climbing with tendrils and have lobed or divided leaves with a long, hollow petiole, while the stems and leaves contain juicy sap (4, 5). *Cucumis* species display either monoecious (separate male and female flowers on the same plant) or andromonoecious (male and hermaphroditic flowers on the same plant) reproductive systems (6). The fruits exhibit

considerable variation in size, shape, texture and flavor, with several species serving as important food crops for human consumption (7). The economic and ecological importance of *Cucumis* cannot be overstated. Cultivated species like melon and cucumber are vital to global food security, while wild relatives serve as reservoirs of genetic diversity for crop improvement programmes, offering traits such as disease resistance and drought tolerance. However, taxonomic uncertainties hinder their full utilization, particularly in regions where wild species are threatened by habitat loss.

Previous taxonomic studies of *Cucumis* in Indonesia have employed phenetic approaches, which classify organisms based on measurable similarities and differences in morphological characteristics (8, 9). While such methods provide valuable preliminary data, they primarily reflect superficial resemblances and may not accurately represent evolutionary relationships among species. Contemporary systematic biology increasingly favors phylogenetic taxonomy and reconstructs evolutionary histories using

molecular data to establish more natural classification system (10, 11). For *Cucumis*, phylogenetic analyses incorporating molecular markers and genomic data have proven particularly valuable for resolving taxonomic uncertainties and refining species classifications (3, 12, 13). This study addresses these challenges by identifying optimal DNA barcodes for *Cucumis*, which will enhance species identification, support conservation efforts and facilitate the use of wild genetic resources in breeding programs worldwide. Phylogenetic analyses utilizing DNA barcodes have emerged as powerful tools for establishing robust classification systems and elucidating evolutionary histories (14–16). The construction of accurate phylogenetic trees for species identification requires standardized DNA sequence segments from specific genomic regions, achievable through DNA barcoding techniques. DNA barcoding employs short, conserved genetic markers to differentiate species by comparing sequences against reference databases. This method has become an essential component of genetic conservation strategies, involving 3 key steps: amplification of target barcode regions through polymerase chain reaction (PCR), DNA sequencing and computational comparison with authenticated reference sequences (17).

Plant biologists have identified numerous potential DNA barcode regions, including both plastid markers (such as *matK*, *rbcl*, *rpoB*, *rpoC1*, *psbA-trnH* and *trnL-trnF*) and nuclear markers (particularly the internal transcribed spacer regions *ITS1* and *ITS2*) (17). Recent comparative studies have demonstrated the superior performance of ITS markers relative to plastid markers for species identification in various plant groups. For instance, *ITS* sequencing proved more effective than *rbcl* for distinguishing *Nepenthes* species and represented the most reliable identification tool for the taxonomically complex genus *Alpinia* (18, 19). Similarly, *ITS* markers outperformed *rbcl* and *trnL-F* for species classification within the *Zingiberaceae* family (20). Nevertheless, plastid markers remain widely used, with *rbcl* serving as a key marker for phylogenetic studies of *Myriostachya wightiana* and combined *matK/rbcl* barcodes successfully identifying Jewel orchid species (21, 22). Optimal barcode selection appears taxon-specific, as evidenced by studies showing that *ITS2* combined with *psbA-trnH* works best for *Rehmannia* species, while a 3-marker combination (*rbcl* + *matK* + *psbA-trnH*) yielded the most robust phylogenetic trees in tropical cloud forest communities (23, 24). Such DNA barcoding approaches enable efficient and reliable species identification across diverse plant groups (25). Despite the growing application of DNA barcoding in plant systematics, its implementation in *Cucumis* research has remained relatively limited, focusing primarily on *rbcl* and *matK* markers for species differentiation and evolutionary studies (26, 27). This investigation aimed to evaluate multiple potential barcode markers (*matK*, *rbcl* and *nrDNA*) through computational analyses to identify the most suitable genetic loci for DNA barcoding. By employing an *in silico* approach, we sought to establish a foundation for more accurate and efficient species identification, which will benefit global efforts in biodiversity conservation, crop improvement and sustainable agriculture.

## Materials and Methods

### Sequence acquisition and processing

Publicly available DNA sequences of *Cucumis* L. species were obtained from the nucleotide databases maintained by the National Center for Biotechnology Information (NCBI) (<https://www.ncbi.nlm.nih.gov/nucleotide/>, accessed between September and November 2024). Sequences were filtered using the criteria “complete CDS” and “type material” (i.e., sequences derived from verified type specimens, when available). NCBI accession numbers provide permanent identifiers for all sequence data, allowing exact replication of dataset by any researcher at any time. Three standard plant DNA barcode regions were selected: the chloroplast-encode *maturase K* (*matK*), *ribulose-1,5-bisphosphate carboxylase/oxygenase large subunit* (*rbcl*) and the *nuclear ribosomal DNA* (*nrDNA*). To ensure data quality, strict inclusion criteria were applied: only sequences with complete coding regions, <1% ambiguous bases and type material where available were considered. To minimize redundancy, sequences were compared using BLASTn and only those with <99% identity to other included sequences were retained. The final dataset included 38 sequences each for the *matK*, *rbcl* and *nrDNA* markers, representing 38 *Cucumis* species. Validated sequences were compiled in FASTA format with standardized headers (Genus\_species\_Gene\_Accession).

### Sequence alignment and phylogenetic reconstruction

Multiple sequence alignments (MSA) were performed using MAFFT v7.511 (<https://mafft.cbrc.jp/alignment/software/>) with the --auto option, gap opening penalty set to 1.53 and 200PAM/k=2 scoring matrix. These alignment parameters represent established standards in phylogenetic analysis and are fully documented in the MAFFT software manual. Alignments were conducted separately for each barcode region (*matK*, *rbcl* and *nrDNA*). The resulting alignments were used for phylogenetic reconstruction using MEGA 11 (<https://www.megasoftware.net/>). Phylogenetic trees were constructed using the Neighbor-Joining (NJ) method with Kimura 2-parameter (K2P) substitution model, a widely accepted approach for DNA barcode analyses. No explicit model selection was performed and K2P was chosen a priori based on established practice in plant molecular phylogenetics. Node support was assessed with 1000 bootstrap replicates and support values interpreted using conventional thresholds: ≥ 70 % (strong support), 50 - 70 % (moderate support) and < 50 % (weak or unsupported). All phylogenetic trees were visualized and exported using MEGA's tree explorer module.

### Genetic diversity analysis

Sequence length and GC content (in %) were calculated using an online GC content calculator ([https://jamiemcgowan.ie/bioinf/gc\\_content.html](https://jamiemcgowan.ie/bioinf/gc_content.html)). All analyses were based on the entire aligned sequences and gap characters were treated as missing data unless otherwise specified. Genetic diversity parameters were estimated using DnaSP v6.12.03 (<http://www.ub.edu/dnasp/>). The following indices were computed: number of nucleotide sites, number of gaps or missing data, number of parsimony-informative sites, total number of mutations, nucleotide diversity ( $\pi$ ), haplotype diversity ( $H_d$ )

and the number of haplotypes. Nucleotide and haplotype diversity estimates were calculated with 95% confidence intervals. Subsequently, haplotype networks were constructed using PopArt v1.7 (<https://popart.maths.otago.ac.nz/>) under the TCS network interference method, with a 95% connection limit. Gaps were treated as a 5<sup>th</sup> character state, which may influence network topology by preserving indel-based differentiation. All software tools used in this study are widely adopted and cited within the molecular ecology and evolutionary biology communities.

## Results and Discussion

The DNA barcode sequence lengths in *Cucumis* L. species showed notable variation across loci. The *matK* sequences ranged from 765 to 1250 base pairs (bp). The *nrDNA*, specifically comprising the internal transcribed spacer region (*ITS1* + 5.8S + *ITS2*), ranged from 397 to 882 bp. In contrast, *rbcl* sequences displayed a broader length range, from 542 to 1428 bp. These differences in sequence length reflect the inherent structural and functional characteristics of each marker region. While non-coding regions like ITS are typically more variable due to frequent insertions and deletions (indels), in this study *rbcl* exhibited the greatest range in length. This unexpected pattern may reflect a combination of true structural diversity in the *rbcl* gene among *Cucumis* L. species and residual differences in how coding sequences are represented in public databases, even after stringent filtering.

However, the observed ranges are broadly consistent with previous reports in plant DNA barcoding studies (28-30). A total of 589 DNA barcode sequences were retrieved from the NCBI databases. Following a rigorous curation process that excluded redundant and unverifiable entries, the final curated dataset included 114 DNA barcode sequences (38 each for *matK*, *rbcl* and *nrDNA*), representing 38 *Cucumis* species (Table 1). The stringent filtering strategy employed in this study stands in contrast to previous approaches, which retained a larger proportion of sequences, up to 70 % of their sequences (31). This more conservative approach likely contributed to the higher phylogenetic resolution but lower haplotype richness observed herein. Nonetheless, rigorous data curation is essential to ensure the accuracy, reliability and reproducibility of downstream analyses (32). Among the 38 *Cucumis* species analyzed, the *matK* exhibited the lowest GC content, while the *nrDNA* displayed the highest. The average GC content for *matK*, *rbcl* and *nrDNA* were 31.63 %, 42.71 % and 61.70 % respectively (Table 2). The high GC content in *nrDNA* likely reflects the structural constraints related to ribosomal RNA folding and compositional asymmetry between transcribed and non-transcribed spacer regions. The GC content of *matK* in this study (31.63 %) is slightly lower than previously reported values for the Cucurbitaceae family, in which *C. sativus*, *C. hystrix* and *C. melo* were found to have GC contents of 32.8 %, 33.12 % and 36.7% respectively (33). It also differed from the 35.2 % reported for cultivated *C. melo*, suggesting possible variation

**Table 1.** The *matK*, *rbcl* and *nrDNA* sequences of 38 species of *Cucumis* used in the study

<i>Cucumis</i> Species	Accession Number		
	<i>matK</i>	<i>rbcl</i>	<i>nrDNA</i>
<i>Cucumis africanus</i>	KY458065.1	KY434396.1	KY434569.1
<i>Cucumis anguria</i>	JQ412228.1	AF534743.1	AM981125.1
<i>Cucumis asper</i>	DQ785842.1	DQ785826.1	EF091850.1
<i>Cucumis bryoniifolius</i>	DQ536657.1	DQ535798.1	EF091851.1
<i>Cucumis debilis</i>	KY458068.1	KY434400.1	KY434571.1
<i>Cucumis dipsaceus</i>	DQ785844.1	MG999522.1	AM981124.1
<i>Cucumis dipsaceus</i> voucher Kotschy	MG993612.1	MG993619.1	MG993578.1
<i>Cucumis ficifolius</i>	DQ785845.1	DQ785829.1	AM981131.1
<i>Cucumis heptadactylis</i>	DQ785840.1	DQ785830.1	AJ488221.1
<i>Cucumis hirsutus</i>	DQ536658.1	DQ535799.1	EF595877.1
<i>Cucumis humifructus</i>	DQ785841.1	DQ785831.1	EF093514.1
<i>Cucumis hystrix</i>	DQ785846.1	DQ785832.1	EF093515.1
<i>Cucumis indicus</i>	MG993608.1	KY434402.1	HM596909.1
<i>Cucumis javanicus</i>	EF174477.1	EF174479.1	EF174484.1
<i>Cucumis maderaspatanus</i>	KY458071.1	KY434405.1	KY434572.1
<i>Cucumis meeusei</i>	KY458072.1	KY434406.1	AJ488225.1
<i>Cucumis melo</i> cultivar Fadasi	KY458073.1	KY434407.1	KY434613.1
<i>Cucumis melo</i> voucher Eig Zohary	MG993611.1	MG993621.1	MG993584.1
<i>Cucumis melo</i> voucher Telford	MG993614.1	MG993625.1	MG993583.1
<i>Cucumis metuliferus</i>	DQ785849.1	DQ785834.1	AM981119.1
<i>Cucumis myriocarpus</i>	DQ785850.1	DQ785836.1	EF093518.1
<i>Cucumis myriocarpus</i> voucher Meebold	MG993617.1	MG993620.1	MG993581.1
<i>Cucumis picrocarpus</i>	KY458116.1	KY434430.1	MG680633.1
<i>Cucumis prophetarum</i>	DQ785851.1	DQ785837.1	AM981128.1
<i>Cucumis queenslandicus</i>	MG993613.1	KY434432.1	HM596921.1
<i>Cucumis rigidus</i>	MG993610.1	KY434433.1	KY434625.1
<i>Cucumis ritchei</i>	KY458118.1	KY434434.1	KY434626.1
<i>Cucumis sacleuxii</i>	DQ785852.1	DQ785838.1	EF093520.1
<i>Cucumis sagittatus</i>	DQ536661.1	DQ535802.1	EF595896.1
<i>Cucumis setosus</i>	KY458119.1	KY434435.1	HM596929.1
<i>Cucumis silentvalleyi</i>	KY458120.1	KY434436.1	HM596931.1
<i>Cucumis</i> sp. HS-2018b	KY458117.1	KY434431.1	KY434624.1
<i>Cucumis</i> sp. HS-2018c voucher Catarino	KY458069.1	KY434403.1	KY434627.1
<i>Cucumis</i> sp. HS-2018c voucher Leonard	KY458070.1	KY434404.1	KY434628.1
<i>Cucumis</i> sp. HS414	EF174478.1	EF174480.1	EF174483.1
<i>Cucumis umbellatus</i>	MG993606.1	KY434438.1	HM596942.1
<i>Cucumis zambianus</i>	KY458121.1	KY434439.1	KY434630.1
<i>Cucumis zeyherii</i>	DQ536663.1	DQ535803.1	AM981133.1

**Table 2.** GC content of *Cucumis* species-based *matK*, *rbcl* and *nrDNA* locus

<i>Cucumis</i> species	Guanine and Cytosine (GC) content (%)		
	<i>matK</i>	<i>rbcl</i>	<i>nrDNA</i>
<i>Cucumis africanus</i>	32.09	42.79	62.20
<i>Cucumis anguria</i>	32.03	42.30	61.83
<i>Cucumis asper</i>	31.68	42.65	62.46
<i>Cucumis bryoniifolius</i>	31.89	42.75	61.01
<i>Cucumis debilis</i>	30.81	42.94	61.46
<i>Cucumis dipsaceus</i>	31.66	43.35	61.35
<i>Cucumis dipsaceus</i> voucher Kotschy	30.20	41.88	58.10
<i>Cucumis ficifolius</i>	31.96	42.65	61.90
<i>Cucumis heptadactylis</i>	31.68	42.58	61.98
<i>Cucumis hirsutus</i>	32.11	42.56	62.81
<i>Cucumis humifructus</i>	31.52	42.79	61.42
<i>Cucumis hystrix</i>	31.72	42.95	64.12
<i>Cucumis indicus</i>	32.06	42.87	62.93
<i>Cucumis javanicus</i>	31.02	43.39	60.27
<i>Cucumis maderaspatanus</i>	31.94	42.87	65.58
<i>Cucumis meeusei</i>	31.97	42.72	60.96
<i>Cucumis melo</i> cultivar Fadasi	31.25	42.50	58.08
<i>Cucumis melo</i> voucher Eig Zohary	30.40	42.50	58.70
<i>Cucumis melo</i> voucher Telford	31.10	41.42	58.54
<i>Cucumis metuliferus</i>	31.51	42.54	63.23
<i>Cucumis myriocarpus</i>	31.66	42.54	63.20
<i>Cucumis myriocarpus</i> voucher Meebold	30.57	41.61	62.98
<i>Cucumis picrocarpus</i>	31.17	42.86	58.51
<i>Cucumis prophetarum</i>	31.84	42.58	63.14
<i>Cucumis queenslandicus</i>	31.79	42.94	59.33
<i>Cucumis rigidus</i>	32.01	42.72	61.72
<i>Cucumis ritchiei</i>	32.11	43.01	66.07
<i>Cucumis saclexii</i>	31.57	42.94	62.04
<i>Cucumis sagittatus</i>	31.98	42.32	59.81
<i>Cucumis setosus</i>	32.20	43.23	62.82
<i>Cucumis silentvalleyi</i>	31.94	43.16	61.75
<i>Cucumis</i> sp. HS-2018b	30.40	42.57	58.25
<i>Cucumis</i> sp. HS-2018c voucher Catarino	31.94	42.79	64.62
<i>Cucumis</i> sp. HS-2018c voucher Leonard	32.16	43.01	66.31
<i>Cucumis</i> sp. HS414	31.94	43.35	58.84
<i>Cucumis umbellatus</i>	31.95	42.87	62.75
<i>Cucumis zambianus</i>	32.23	42.80	61.94
<i>Cucumis zeyherii</i>	31.97	42.58	61.72

among species or accessions (34). These findings indicate that *nrDNA* is the most informative locus for assessing GC content variation in *Cucumis* L.

Analyses using DnaSP v6.12.03 (Table 3) revealed marked differences in genetic variability across the three barcode loci. Among them, *rbcl* exhibited the lowest values for parsimony informative sites (7 sites), total mutations, nucleotide diversity ( $P_i = 0.00650$ ), haplotype diversity ( $H_d = 0.0879$ ) and haplotype number ( $h = 14$ ) compared to other loci (32). This low variability likely reflects functional constraints, as *rbcl* encodes the rubisco enzyme essential for carbon fixation and is subject to strong purifying selection, thereby limiting the accumulation of mutations (35). In contrast, the *nrDNA* displayed the highest genetic variation, with 57 parsimony-informative sites, 108 total mutations, a high haplotype diversity ( $H_d = 0.996$ ) and a moderate nucleotide diversity ( $P_i = 0.04344$ ). As *nrDNA* comprises the internal transcribed spacer

region, non-coding and under less evolutionary constraints, it tends to evolve more rapidly (36). This leads to the accumulation of mutations over shorter evolutionary timescales. The observed diversity suggests a recent population expansion (37). The highest number of parsimony-informative sites in *nrDNA* reinforces its utility for species-level discrimination. The *matK* locus displayed intermediate levels of diversity, with 23 parsimony-informative sites, 56 total mutations, a high haplotype diversity ( $H_d = 0.982$ ) and a moderate nucleotide diversity ( $P_i = 0.01598$ ). This suggests that *matK* can complement *nrDNA* for phylogenetic resolution, albeit with lower variability. Phylogenetic relationships among *Cucumis* species were inferred using MEGA 11, following the Tamura methodological framework with modifications in bootstrap algorithm selection (38). To root the phylogenetic tree, *Arabidopsis thaliana* and *Oryza sativa* were employed as outgroups, aligning with previous phylogenetic studies (39).

**Table 3.** Characterization of *Cucumis* species-based *matK*, *rbcl* and *nrDNA* locus

Data	<i>matK</i>	<i>rbcl</i>	<i>nrDNA</i>
Number of sites	1275	1459	949
Gaps/missing data	842	970	584
Parsimony informative site	23	7	57
Total number of mutation	56	32	108
Nucleotide diversity ( $P_i$ )	0.01598	0.00650	0.04344
Haplotype diversity ( $H_d$ )	0.982	0.879	0.996
Number of haplotypes ( $h$ )	30	14	35



The *matK*-based phylogenetic tree resolved 2 major clades within *Cucumis* L., with *A. thaliana* and *O. sativa* serving as reference outgroups (Fig. 1). The observed divergence between these clades corresponds to paleopolyploidization events in Cucurbitaceae ancestry, followed by diploidization processes that shaped distinct evolutionary trajectories (40). The first clade comprised of *C. picrocarpus*, *C. sp. HS-2018b*, *C. dipsaceus* voucher Kotschy, *C. melo* (cultivars Fadasi, voucher Eig Zohary and voucher Telford), suggesting a close evolutionary relationship among these taxa. Their clustering may reflect strong artificial selection during domestication, with genetic bottlenecks reducing diversity at both neutral and functional loci. This grouping partially contradicts the prior classification but aligns with the recent combined nuclear and plastid sequence (4, 41, 42). The second clade encompassed a more diverse group of *Cucumis* species, including *C. javanicus*, *C. umbellatus*, *C. sp. HS414*, *C. queenslandicus*, *C. silentvalleyi*, *C. setosus*, *C. indicus*, *C. debilis*, *C. hystrix*, *C. sp. HS-2018c* (vouchers Leonard and vouchers Catarino), *C. ritchiei*, *C. maderaspatanus*, *C. metuliferus*, *C. saclexii*, *C. sagittatus*, *C. dipsaceus*, *C. prophetarum*, *C. meeusei*, *C. ficifolius*, *C. zambianus*, *C. rigidus*, *C. africanus*, *C. zeyherii*, *C. heptadactylis*, *C. anguria*, *C. myriocarpus* (including voucher Meebold), *C. asper*, *C. hirsutus*, *C. humifructus* and *C. bryoniifolius*. The consistent placement of *C. melo* and *C. myriocarpus* within their respective clades supports the reliability of the *matK* locus for phylogenetic inference in *Cucumis* L. These results align with previous studies demonstrating the effectiveness of the *matK* barcode in discriminating closely related species within the Cucurbitaceae, including *Momordica* and *C. melo* (26, 43). Phylogenetic analysis based on the *rbcl* locus (Fig. 2) provided a robust framework for *Cucumis* L. phylogeny, as *A. thaliana* and *O. sativa* formed a distinct clade separate from the remaining *Cucumis* L. species. *C. javanicus* was positioned as a basal taxon within the *Cucumis* clade, rather than clustering more closely with *A. thaliana*. The *rbcl* gene, encoding the Rubisco enzyme, has been widely used as a plastid marker to resolve phylogenetic relationships at the generic and specific levels (44). The phylogenetic tree revealed that *C. melo* formed a well-supported clade with *C. picrocarpus*, *C. sp. HS-2018b* and *C. dipsaceus* voucher Kotschy, reflecting their close evolutionary relationship. While *rbcl* exhibited strong discriminatory power at the species level, it showed limited resolution for distinguishing cultivars or vouchers within *C. melo*. These findings reinforce previous research highlighting *rbcl* as a reliable barcode marker, although its lower evolutionary rate compared to *matK* may constrain its ability to resolve recently diverged taxa (45, 46).

The phylogenetic tree inferred from the *nrDNA* locus (Fig. 3) exhibited superior discriminatory power and resolution compared to *matK* and *rbcl*, with *A. thaliana* and *O. sativa* clearly positioned as outgroups. Several species formed distinct subclades, facilitating the elucidation of evolutionary relationships. Notably, *C. melo* voucher Telford, *C. melo* voucher Eig Zohary, *C. melo* cultivar Fadasi, *C. sp. HS-2018b*, *C. picrocarpus* and *C. dipsaceus* voucher Kotschy clustered closely, suggesting a strong phylogenetic relationship. Similarly, *C. indicus*, *C. setosus*, *C. silentvalleyi*,

*C. sagittatus*, *C. ritchiei*, *C. maderaspatanus*, *C. sp. HS-2018c* (voucher Catarino and voucher Leonard) formed a distinct phylogenetic clade. Another major clade comprised *C. africanus*, *C. zambianus*, *C. heptadactylis*, *C. prophetarum*, *C. rigidus*, *C. meeusei*, *C. ficifolius*, *C. zeyherii*, *C. dipsaceus*, *C. anguria*, *C. myriocarpus* (including voucher Meebold). Interestingly, *C. dipsaceus* and *C. dipsaceus* voucher Kotschy exhibited a significant phylogenetic distance, suggesting potential misidentification for one or both accessions based on *matK*, *rbcl* and *nrDNA* data. The *nrDNA*-based phylogeny demonstrated exceptional resolution at the intraspecific level within *Cucumis* L. compared to *matK* and *rbcl*. The superior performance of *nrDNA* is likely due to the conserved nature of the 5.8S region and the higher variability of the *ITS* region, which has been shown to be effective in discriminating closely related species (47). Consistent with these findings, previous studies have reported higher mutation rates and informative sites in the *ITS* and *ITS2* regions of *Rehmannia* species compared to *matK* and *rbcl* (23).

The total genetic distance for the *matK* gene, calculated using the Tamura-3-parameter model (Table 4), ranged from a low of 0.012 to 0.030. Several species, including *C. sagittatus*, *C. heptadactylis*, *C. ficifolius*, *C. africanus*, *C. maderaspatanus*, *C. setosus* and *C. dipsaceus* (including voucher Kotschy) exhibited identical genetic distances of 0.020 at this locus. The *rbcl* gene displayed a broader genetic distance range (0.009-0.088; Table 5), with *C. javanicus* (0.088) clearly differentiated from the remaining taxa. In contrast, the *nrDNA* region demonstrated the highest genetic variation among the 3 markers, with distances spanning from 0.008 to 0.097 (Table 6). These distances are 80 % higher than those reported for the same markers in the sister genus *Vanda*, reflecting different evolutionary rates between these lineages (48). TCS-based haplotype networks (Fig. 4) revealed shared haplotypes among species. A total of 30 distinct *matK* haplotypes were identified (Fig. 4a). Table 7 shows haplotype distribution among specific species, with *C. heptadactylis*, *C. anguria* and *C. myriocarpus* (including voucher Meebold) sharing Hap\_5; *C. sp. HS-2018c* voucher Leonard and *C. maderaspatanus* sharing Hap\_19; *C. meeusei*, *C. zambianus* and *C. rigidus* sharing Hap\_20; and *C. melo* (cultivar Fadasi and voucher Eig Zohary) and *C. dipsaceus* voucher Kotschy sharing Hap\_21. Hap\_5 was found in 4 samples and Hap\_19 in 2, while Hap\_20 and Hap\_21 were each found in 3 samples. The *rbcl* haplotype network (Fig. 4b) indicated that Hap\_9 was the ancestral haplotype for Hap\_3 and Hap\_7, with fewer mutational steps to Hap\_3. Hap\_1 represented a lineage with a higher number of mutations. This pattern was consistent with species distribution, as *C. hirsutus*, *C. heptadactylis*, *C. hystrix* and *C. prophetarum* shared Hap\_3, while *C. ficifolius*, *C. humifructus*, *C. myriocarpus*, *C. africanus*, *C. sp. HS-2018c* voucher Leonard, *C. maderaspatanus*, *C. ritchiei*, *C. setosus*, *C. silentvalleyi* and *C. myriocarpus* voucher Meebold shared Hap\_7 (Table 7). The *nrDNA* haplotype network (Fig. 4c) showed that *C. myriocarpus* (including voucher Meebold) shared Hap\_12 and *C. sp. HS-2018b* and *C. picrocarpus* shared Hap\_27 (Table 7). The clustering of these haplotypes reflects historical biogeographic events that shaped *Cucumis* L. diversification, as noted in Cucurbitaceae phylogeographic studies (49).

**Table 4.** Total genetic distance between *Cucumis* L. species using *matK*

	1	2	3	4	5	6	7	8	9	10	11	12	13	14	15	16	17	18	19	20	21	22	23	24	25	26	27	28	29	30	31	32	33	34	35	36	37	38	
<i>C. boryanifolius</i>	-	-	-	-	-	-	-	-	-	-	-	-	-	-	-	-	-	-	-	-	-	-	-	-	-	-	-	-	-	-	-	-	-	-	-	-	-	-	-
<i>C. hirsutus</i>	0.024	-	-	-	-	-	-	-	-	-	-	-	-	-	-	-	-	-	-	-	-	-	-	-	-	-	-	-	-	-	-	-	-	-	-	-	-	-	
<i>C. sagittatus</i>	0.020	0.024	-	-	-	-	-	-	-	-	-	-	-	-	-	-	-	-	-	-	-	-	-	-	-	-	-	-	-	-	-	-	-	-	-	-	-	-	
<i>C. seyerii</i>	0.023	0.027	0.020	-	-	-	-	-	-	-	-	-	-	-	-	-	-	-	-	-	-	-	-	-	-	-	-	-	-	-	-	-	-	-	-	-	-	-	
<i>C. heptadactylis</i>	0.020	0.024	0.018	0.003	-	-	-	-	-	-	-	-	-	-	-	-	-	-	-	-	-	-	-	-	-	-	-	-	-	-	-	-	-	-	-	-	-	-	
<i>C. humifusus</i>	0.025	0.011	0.024	0.025	0.021	-	-	-	-	-	-	-	-	-	-	-	-	-	-	-	-	-	-	-	-	-	-	-	-	-	-	-	-	-	-	-	-	-	
<i>C. asper</i>	0.012	0.024	0.018	0.023	0.019	0.023	-	-	-	-	-	-	-	-	-	-	-	-	-	-	-	-	-	-	-	-	-	-	-	-	-	-	-	-	-	-	-	-	
<i>C. dipsacensis</i>	0.020	0.023	0.018	0.004	0.002	0.020	0.018	-	-	-	-	-	-	-	-	-	-	-	-	-	-	-	-	-	-	-	-	-	-	-	-	-	-	-	-	-	-	-	
<i>C. feffolius</i>	0.020	0.024	0.018	0.006	0.003	0.021	0.020	0.003	-	-	-	-	-	-	-	-	-	-	-	-	-	-	-	-	-	-	-	-	-	-	-	-	-	-	-	-	-	-	
<i>C. lychnis</i>	0.021	0.022	0.017	0.019	0.016	0.022	0.021	0.016	0.016	-	-	-	-	-	-	-	-	-	-	-	-	-	-	-	-	-	-	-	-	-	-	-	-	-	-	-	-	-	
<i>C. menispermus</i>	0.022	0.024	0.019	0.018	0.015	0.024	0.020	0.015	0.016	0.018	-	-	-	-	-	-	-	-	-	-	-	-	-	-	-	-	-	-	-	-	-	-	-	-	-	-	-	-	
<i>C. myriocarpus</i>	0.021	0.025	0.018	0.003	0.001	0.021	0.020	0.002	0.004	0.017	0.016	-	-	-	-	-	-	-	-	-	-	-	-	-	-	-	-	-	-	-	-	-	-	-	-	-	-	-	
<i>C. prophanum</i>	0.022	0.025	0.019	0.006	0.003	0.023	0.021	0.003	0.005	0.019	0.017	0.004	-	-	-	-	-	-	-	-	-	-	-	-	-	-	-	-	-	-	-	-	-	-	-	-	-	-	
<i>C. socinensis</i>	0.024	0.026	0.021	0.020	0.017	0.025	0.022	0.017	0.017	0.018	0.003	0.018	0.019	-	-	-	-	-	-	-	-	-	-	-	-	-	-	-	-	-	-	-	-	-	-	-	-	-	-
<i>C. juncatus</i>	0.026	0.032	0.026	0.028	0.025	0.030	0.028	0.025	0.025	0.016	0.029	0.026	0.028	0.030	-	-	-	-	-	-	-	-	-	-	-	-	-	-	-	-	-	-	-	-	-	-	-	-	-
<i>C. so HS414</i>	0.030	0.034	0.027	0.027	0.026	0.034	0.023	0.026	0.027	0.017	0.029	0.027	0.028	0.012	-	-	-	-	-	-	-	-	-	-	-	-	-	-	-	-	-	-	-	-	-	-	-	-	-
<i>C. angustata</i>	0.022	0.027	0.019	0.003	0.000	0.025	0.020	0.003	0.005	0.019	0.017	0.000	0.003	0.020	0.030	0.032	-	-	-	-	-	-	-	-	-	-	-	-	-	-	-	-	-	-	-	-	-	-	-
<i>C. affinis</i>	0.020	0.023	0.018	0.004	0.001	0.023	0.019	0.003	0.004	0.017	0.015	0.002	0.004	0.016	0.028	0.028	0.001	-	-	-	-	-	-	-	-	-	-	-	-	-	-	-	-	-	-	-	-	-	-
<i>C. debilis</i>	0.015	0.019	0.013	0.015	0.013	0.019	0.017	0.013	0.013	0.003	0.016	0.014	0.015	0.016	0.009	0.013	0.013	0.015	-	-	-	-	-	-	-	-	-	-	-	-	-	-	-	-	-	-	-	-	-
<i>C. so HS-2018c voucher Catarino</i>	0.022	0.025	0.018	0.021	0.019	0.026	0.022	0.019	0.019	0.008	0.021	0.019	0.020	0.021	0.019	0.020	0.018	0.020	0.006	-	-	-	-	-	-	-	-	-	-	-	-	-	-	-	-	-	-	-	-
<i>C. so HS-2018c voucher Leonard</i>	0.021	0.025	0.018	0.022	0.019	0.026	0.021	0.019	0.020	0.008	0.021	0.020	0.020	0.021	0.017	0.018	0.016	0.020	0.006	0.004	-	-	-	-	-	-	-	-	-	-	-	-	-	-	-	-	-	-	-
<i>C. madrocarpus</i>	0.020	0.023	0.016	0.019	0.017	0.024	0.020	0.017	0.018	0.006	0.019	0.018	0.019	0.019	0.017	0.018	0.016	0.018	0.003	0.002	0.002	-	-	-	-	-	-	-	-	-	-	-	-	-	-	-	-	-	-
<i>C. meiselii</i>	0.018	0.021	0.015	0.006	0.004	0.020	0.018	0.004	0.004	0.014	0.012	0.004	0.004	0.013	0.026	0.024	0.005	0.005	0.012	0.017	0.017	0.015	-	-	-	-	-	-	-	-	-	-	-	-	-	-	-	-	
<i>C. melo culinar Fadas</i>	0.023	0.029	0.019	0.024	0.021	0.027	0.022	0.021	0.022	0.016	0.024	0.022	0.023	0.024	0.025	0.028	0.022	0.023	0.022	0.023	0.023	0.015	0.020	-	-	-	-	-	-	-	-	-	-	-	-	-	-	-	-
<i>C. pterocarpus</i>	0.025	0.030	0.023	0.027	0.025	0.028	0.025	0.025	0.025	0.019	0.026	0.025	0.026	0.026	0.027	0.029	0.026	0.026	0.014	0.020	0.019	0.018	0.022	0.004	-	-	-	-	-	-	-	-	-	-	-	-	-	-	-
<i>C. so HS-2018b</i>	0.019	0.025	0.019	0.021	0.019	0.023	0.020	0.019	0.019	0.015	0.022	0.020	0.021	0.024	0.021	0.025	0.018	0.021	0.012	0.017	0.017	0.015	0.020	0.002	0.002	-	-	-	-	-	-	-	-	-	-	-	-	-	-
<i>C. rufus</i>	0.023	0.026	0.019	0.022	0.019	0.027	0.023	0.019	0.020	0.009	0.022	0.020	0.021	0.022	0.019	0.019	0.019	0.021	0.006	0.004	0.004	0.003	0.018	0.018	0.020	0.017	-	-	-	-	-	-	-	-	-	-	-	-	-
<i>C. setosus</i>	0.020	0.024	0.018	0.021	0.019	0.025	0.019	0.017	0.019	0.009	0.021	0.019	0.020	0.021	0.018	0.021	0.020	0.020	0.005	0.010	0.010	0.008	0.017	0.018	0.021	0.016	0.011	-	-	-	-	-	-	-	-	-	-	-	
<i>C. siamensis</i>	0.023	0.027	0.019	0.024	0.021	0.028	0.020	0.019	0.022	0.011	0.024	0.022	0.023	0.024	0.020	0.021	0.025	0.022	0.008	0.011	0.011	0.010	0.019	0.019	0.023	0.019	0.012	0.009	-	-	-	-	-	-	-	-	-	-	
<i>C. zambianus</i>	0.021	0.027	0.019	0.008	0.005	0.025	0.021	0.005	0.006	0.020	0.018	0.006	0.006	0.006	0.020	0.028	0.030	0.001	0.006	0.015	0.021	0.021	0.019	0.007	0.024	0.027	0.022	0.021	0.023	-	-	-	-	-	-	-	-	-	
<i>C. umbellatus</i>	0.029	0.031	0.027	0.028	0.025	0.033	0.028	0.025	0.026	0.014	0.026	0.026	0.026	0.026	0.014	0.010	0.027	0.027	0.015	0.019	0.017	0.017	0.024	0.029	0.031	0.030	0.018	0.020	0.020	0.030	-	-	-	-	-	-	-	-	
<i>C. indicus</i>	0.024	0.025	0.019	0.023	0.020	0.026	0.022	0.019	0.021	0.010	0.021	0.021	0.022	0.021	0.020	0.022	0.022	0.022	0.007	0.011	0.011	0.009	0.019	0.019	0.022	0.018	0.011	0.010	0.011	0.023	0.021	-	-	-	-	-	-	-	
<i>C. rigidus</i>	0.017	0.022	0.016	0.005	0.003	0.021	0.018	0.003	0.004	0.016	0.014	0.004	0.004	0.016	0.026	0.027	0.003	0.004	0.012	0.017	0.017	0.016	0.003	0.020	0.023	0.019	0.018	0.017	0.019	0.005	0.026	0.019	-	-	-	-	-	-	
<i>C. melo voucher Ele Zohary</i>	0.021</																																						

**Table 5.** Total genetic distance between *Cucumis* L. species using *rbcL*

	1	2	3	4	5	6	7	8	9	10	11	12	13	14	15	16	17	18	19	20	21	22	23	24	25	26	27	28	29	30	31	32	33	34	35	36	37	38
<i>C. anguria</i>	-	-	-	-	-	-	-	-	-	-	-	-	-	-	-	-	-	-	-	-	-	-	-	-	-	-	-	-	-	-	-	-	-	-	-	-	-	-
<i>C. bryoniaefolius</i>	0.013	-	-	-	-	-	-	-	-	-	-	-	-	-	-	-	-	-	-	-	-	-	-	-	-	-	-	-	-	-	-	-	-	-	-	-	-	-
<i>C. hirsutus</i>	0.014	0.003	-	-	-	-	-	-	-	-	-	-	-	-	-	-	-	-	-	-	-	-	-	-	-	-	-	-	-	-	-	-	-	-	-	-	-	-
<i>C. sagittatus</i>	0.014	0.005	0.006	-	-	-	-	-	-	-	-	-	-	-	-	-	-	-	-	-	-	-	-	-	-	-	-	-	-	-	-	-	-	-	-	-	-	-
<i>C. segeterii</i>	0.010	0.005	0.007	0.007	-	-	-	-	-	-	-	-	-	-	-	-	-	-	-	-	-	-	-	-	-	-	-	-	-	-	-	-	-	-	-	-	-	-
<i>C. asper</i>	0.014	0.002	0.004	0.005	0.006	-	-	-	-	-	-	-	-	-	-	-	-	-	-	-	-	-	-	-	-	-	-	-	-	-	-	-	-	-	-	-	-	-
<i>C. flexilis</i>	0.010	0.004	0.006	0.006	0.002	0.005	-	-	-	-	-	-	-	-	-	-	-	-	-	-	-	-	-	-	-	-	-	-	-	-	-	-	-	-	-	-	-	-
<i>C. hystrix</i>	0.009	0.004	0.005	0.005	0.001	0.004	0.001	-	-	-	-	-	-	-	-	-	-	-	-	-	-	-	-	-	-	-	-	-	-	-	-	-	-	-	-	-	-	-
<i>C. hystrix</i>	0.015	0.004	0.002	0.007	0.007	0.004	0.003	0.006	-	-	-	-	-	-	-	-	-	-	-	-	-	-	-	-	-	-	-	-	-	-	-	-	-	-	-	-	-	-
<i>C. hystrix</i>	0.017	0.006	0.006	0.007	0.008	0.009	0.007	0.007	0.008	-	-	-	-	-	-	-	-	-	-	-	-	-	-	-	-	-	-	-	-	-	-	-	-	-	-	-	-	-
<i>C. metulifolius</i>	0.015	0.007	0.007	0.008	0.009	0.006	0.003	0.007	0.009	0.008	-	-	-	-	-	-	-	-	-	-	-	-	-	-	-	-	-	-	-	-	-	-	-	-	-	-	-	-
<i>C. myriocarpus</i>	0.012	0.007	0.009	0.009	0.005	0.008	0.003	0.004	0.008	0.012	0.011	-	-	-	-	-	-	-	-	-	-	-	-	-	-	-	-	-	-	-	-	-	-	-	-	-	-	-
<i>C. prophanum</i>	0.009	0.004	0.005	0.005	0.001	0.004	0.001	0.000	0.006	0.007	0.007	0.004	-	-	-	-	-	-	-	-	-	-	-	-	-	-	-	-	-	-	-	-	-	-	-	-	-	-
<i>C. saraceni</i>	0.018	0.009	0.009	0.010	0.011	0.008	0.010	0.010	0.011	0.007	0.008	0.013	0.010	-	-	-	-	-	-	-	-	-	-	-	-	-	-	-	-	-	-	-	-	-	-	-	-	-
<i>C. juncatus</i>	0.008	0.001	0.009	0.002	0.009	0.003	0.003	0.001	0.008	0.008	0.005	0.002	0.001	0.009	-	-	-	-	-	-	-	-	-	-	-	-	-	-	-	-	-	-	-	-	-	-	-	-
<i>C. sp. HS414</i>	0.015	0.004	0.005	0.007	0.008	0.004	0.007	0.006	0.006	0.007	0.008	0.010	0.006	0.011	0.003	-	-	-	-	-	-	-	-	-	-	-	-	-	-	-	-	-	-	-	-	-	-	-
<i>C. officinalis</i>	0.010	0.004	0.006	0.005	0.002	0.005	0.000	0.001	0.005	0.007	0.008	0.000	0.001	0.010	0.077	0.007	-	-	-	-	-	-	-	-	-	-	-	-	-	-	-	-	-	-	-	-	-	-
<i>C. dehis</i>	0.016	0.006	0.006	0.007	0.008	0.007	0.007	0.007	0.008	0.006	0.008	0.007	0.007	0.010	0.083	0.007	0.007	-	-	-	-	-	-	-	-	-	-	-	-	-	-	-	-	-	-	-	-	-
<i>C. inderis</i>	0.014	0.003	0.003	0.005	0.007	0.004	0.006	0.005	0.005	0.004	0.007	0.006	0.005	0.009	0.080	0.004	0.006	0.004	-	-	-	-	-	-	-	-	-	-	-	-	-	-	-	-	-	-	-	-
<i>C. sp. HS-2018c voucher Catarino</i>	0.014	0.004	0.004	0.004	0.007	0.005	0.006	0.005	0.007	0.004	0.007	0.006	0.005	0.009	0.082	0.003	0.006	0.004	0.003	-	-	-	-	-	-	-	-	-	-	-	-	-	-	-	-	-	-	-
<i>C. sp. HS-2018c voucher Leonard</i>	0.014	0.004	0.004	0.005	0.007	0.005	0.004	0.005	0.005	0.004	0.007	0.004	0.005	0.009	0.081	0.003	0.004	0.004	0.003	0.003	-	-	-	-	-	-	-	-	-	-	-	-	-	-	-	-	-	-
<i>C. madrocarpus</i>	0.016	0.006	0.006	0.007	0.008	0.007	0.006	0.007	0.007	0.006	0.008	0.006	0.007	0.010	0.082	0.007	0.006	0.006	0.004	0.004	0.003	-	-	-	-	-	-	-	-	-	-	-	-	-	-	-	-	-
<i>C. melalei</i>	0.009	0.004	0.005	0.004	0.001	0.004	0.001	0.000	0.006	0.007	0.007	0.001	0.000	0.010	0.077	0.006	0.001	0.007	0.005	0.005	0.005	0.007	-	-	-	-	-	-	-	-	-	-	-	-	-	-	-	-
<i>C. melo culinar Fadas</i>	0.017	0.006	0.007	0.008	0.010	0.008	0.009	0.008	0.010	0.009	0.010	0.009	0.008	0.012	0.085	0.010	0.009	0.009	0.007	0.007	0.007	0.009	0.008	-	-	-	-	-	-	-	-	-	-	-	-	-	-	-
<i>C. picrocarpus voucher Telford</i>	0.018	0.010	0.010	0.011	0.012	0.010	0.011	0.010	0.012	0.011	0.012	0.011	0.010	0.014	0.081	0.012	0.011	0.011	0.010	0.010	0.010	0.011	0.010	0.005	-	-	-	-	-	-	-	-	-	-	-	-	-	-
<i>C. sp. HS-2018b</i>	0.016	0.006	0.006	0.007	0.008	0.007	0.007	0.007	0.008	0.007	0.008	0.007	0.007	0.010	0.083	0.003	0.007	0.007	0.006	0.006	0.006	0.007	0.007	0.001	0.004	-	-	-	-	-	-	-	-	-	-	-	-	-
<i>C. guineensis</i>	0.014	0.003	0.004	0.005	0.007	0.003	0.006	0.005	0.005	0.006	0.007	0.006	0.005	0.010	0.079	0.001	0.006	0.006	0.003	0.004	0.004	0.006	0.005	0.009	0.011	0.007	-	-	-	-	-	-	-	-	-	-	-	-
<i>C. rigidus</i>	0.009	0.004	0.005	0.004	0.001	0.004	0.001	0.000	0.006	0.007	0.007	0.001	0.000	0.010	0.077	0.006	0.001	0.007	0.005	0.005	0.005	0.007	0.000	0.008	0.010	0.007	0.005	-	-	-	-	-	-	-	-	-	-	-
<i>C. rufus</i>	0.014	0.004	0.004	0.005	0.007	0.005	0.004	0.005	0.005	0.004	0.007	0.004	0.005	0.009	0.081	0.003	0.004	0.004	0.003	0.003	0.001	0.003	0.005	0.007	0.010	0.006	0.004	0.005	-	-	-	-	-	-	-	-	-	-
<i>C. sepius</i>	0.016	0.005	0.005	0.007	0.009	0.006	0.007	0.007	0.006	0.007	0.009	0.007	0.007	0.011	0.081	0.006	0.007	0.007	0.004	0.005	0.004	0.005	0.007	0.010	0.012	0.008	0.005	0.007	0.004	-	-	-	-	-	-	-	-	-
<i>C. siamensis</i>	0.016	0.005	0.005	0.007	0.009	0.006	0.007	0.007	0.006	0.007	0.009	0.007	0.007	0.011	0.082	0.003	0.007	0.007	0.004	0.005	0.004	0.005	0.007	0.010	0.012	0.008	0.005	0.007	0.004	0.001	-	-	-	-	-	-	-	-
<i>C. umbellatus</i>	0.014	0.004	0.005	0.006	0.007	0.004	0.006	0.005	0.006	0.007	0.008	0.006	0.005	0.010	0.079	0.002	0.006	0.007	0.004	0.005	0.005	0.007	0.005	0.010	0.012	0.008	0.001	0.005	0.005	0.006	0.006	-	-	-	-	-	-	-
<i>C. zambianus</i>	0.010	0.004	0.006	0.005	0.002	0.004	0.001	0.001	0.007	0.007	0.007	0.001	0.001	0.009	0.078	0.006	0.001	0.007	0.006	0.006	0.006	0.007	0.001	0.009	0.011	0.007	0.005	0.001	0.006	0.008	0.008	0.005	-	-	-	-	-	-
<i>C. dipreus voucher Kotschy</i>	0.015	0.008	0.006	0.007	0.008	0.007	0.007	0.006	0.007	0.006	0.009	0.007	0.006	0.007	0.034	0.010	0.007	0.009	0.006	0.007	0.007	0.007	0.006	0.002	0.000	0.000	0.009	0.006	0.007	0.007	0.009	0.009	0.007	-	-	-	-	-
<i>C. myriocarpus voucher Neesbold</i>	0.009	0.003	0.006	0.002	0.002	0.005	0.000	0.001	0.005	0.006	0.006	0.000	0.001	0.009	0.049	0.006	0.000	0.006	0.005	0.005	0.003	0.003	0.001	0.007	0.006	0.006	0.006	0.001	0.002	0.005	0.005	0.006	0.002	0.007	-	-	-	-
<i>C. melo voucher E. Zohary</i>	0.017	0.006	0.007	0.008	0.010	0.008	0.009	0.008	0.010	0.009	0.010	0.009	0.008	0.012	0.085	0.010	0.009	0.009	0.007	0.007	0.007	0.009	0.008	0.000	0.005	0.001	0.009	0.008	0.007	0.010	0.010	0.010	0.009	0.002	0.007	-	-	-
<i>C. melo voucher Telford</i>	0.013	0.006	0.008	0.007	0.007	0.010	0.007	0.006	0.012	0.008	0.008	0.007	0.006	0.012	0.055	0.012	0.007	0.008	0.007	0.007	0.007	0.008	0.006	0.000	0.001	0.001	0.011	0.006	0.007	0.010	0.010	0.011	0.007	0.002	0.000	-	-	-
<i>C. dipreus</i>	0.010	0.004	0.006	0.005	0.002	0.005	0.001	0.000	0.006	0.007	0.008	0.001	0.000	0.010	0.071	0.006	0.001	0.006	0.005	0.006	0.006	0.007	0.000	0.009	0.011	0.007	0.006	0.000	0.000	0.008	0.008	0.006	0.001	0.006	0.001	0.009	0.006	-

**Table 6.** Total genetic distance between *Cucumis* L. species using *nrDNA*

	1	2	3	4	5	6	7	8	9	10	11	12	13	14	15	16	17	18	19	20	21	22	23	24	25	26	27	28	29	30	31	32	33	34	35	36	37	38	
<i>C. heterodoxus</i>	-	-	-	-	-	-	-	-	-	-	-	-	-	-	-	-	-	-	-	-	-	-	-	-	-	-	-	-	-	-	-	-	-	-	-	-	-	-	-
<i>C. meiselae</i>	0.015	-	-	-	-	-	-	-	-	-	-	-	-	-	-	-	-	-	-	-	-	-	-	-	-	-	-	-	-	-	-	-	-	-	-	-	-	-	
<i>C. menispermus</i>	0.032	0.030	-	-	-	-	-	-	-	-	-	-	-	-	-	-	-	-	-	-	-	-	-	-	-	-	-	-	-	-	-	-	-	-	-	-	-	-	
<i>C. dipaxensis</i>	0.033	0.031	0.038	-	-	-	-	-	-	-	-	-	-	-	-	-	-	-	-	-	-	-	-	-	-	-	-	-	-	-	-	-	-	-	-	-	-	-	
<i>C. angustata</i>	0.020	0.018	0.024	0.018	-	-	-	-	-	-	-	-	-	-	-	-	-	-	-	-	-	-	-	-	-	-	-	-	-	-	-	-	-	-	-	-	-	-	
<i>C. propinqua</i>	0.025	0.023	0.033	0.029	0.014	-	-	-	-	-	-	-	-	-	-	-	-	-	-	-	-	-	-	-	-	-	-	-	-	-	-	-	-	-	-	-	-	-	
<i>C. f.</i>																																							



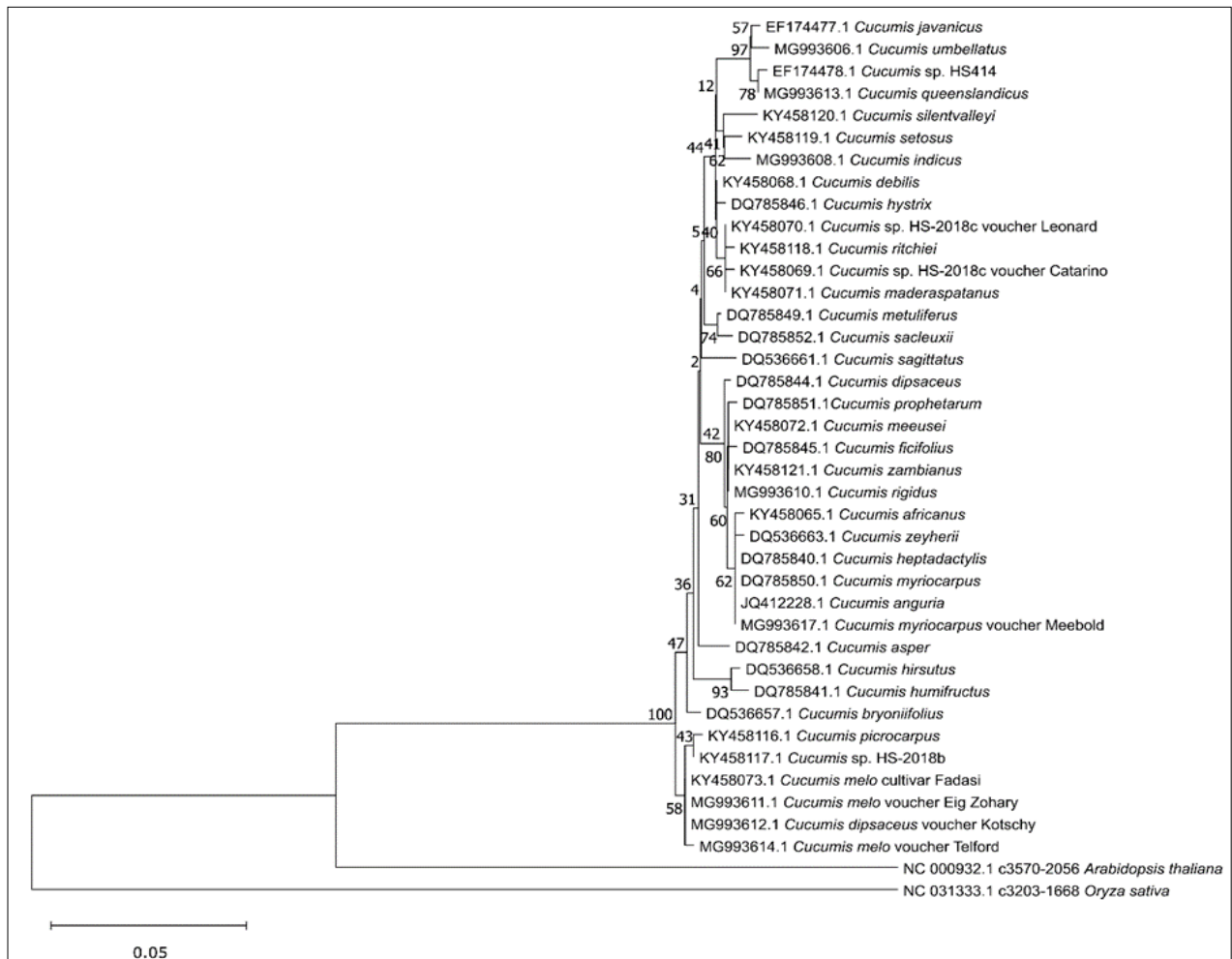


**Fig. 1.** *Cucumis* phylogenetic tree using the *maturase K* barcode (*matK*).

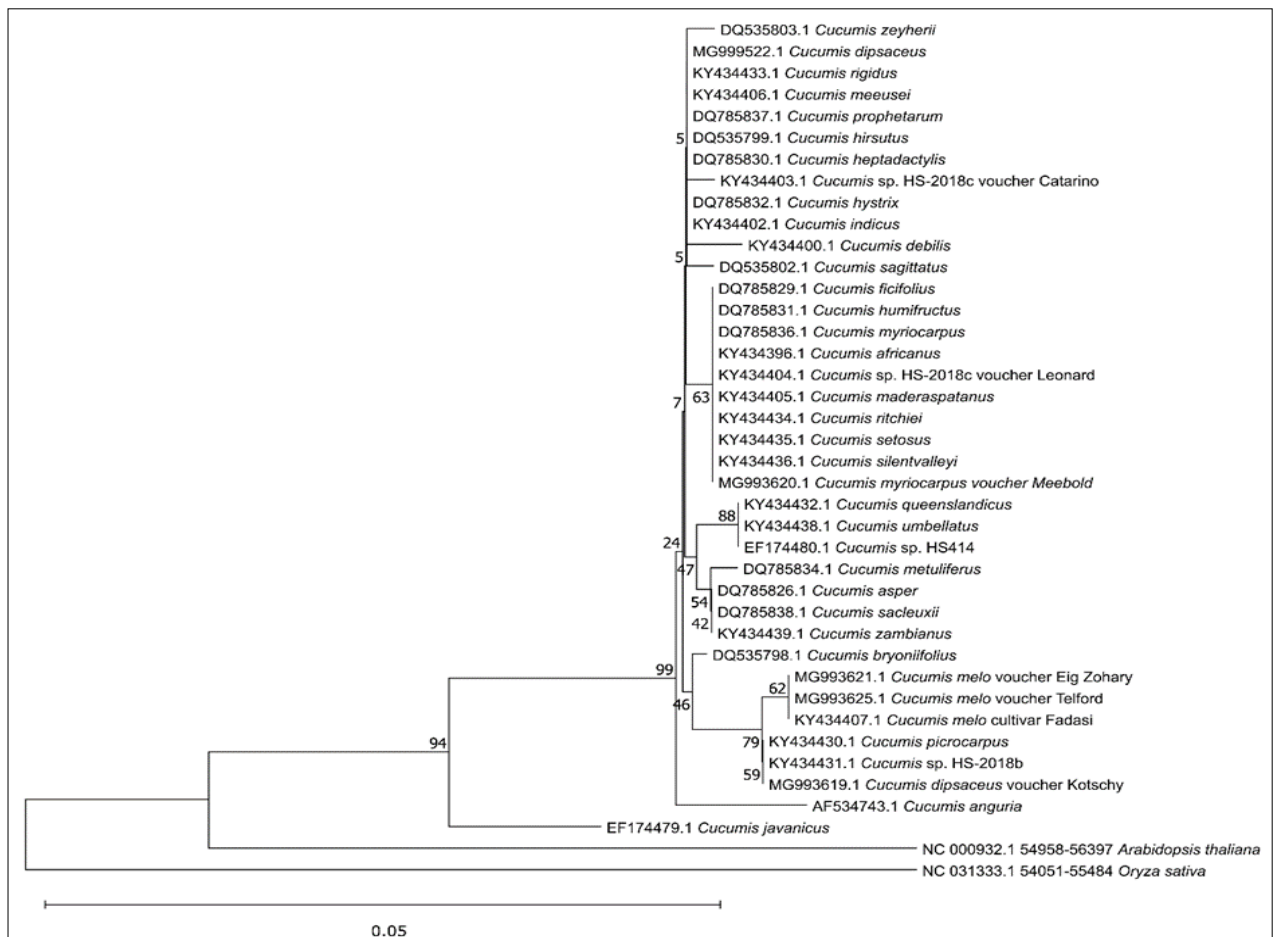


**Fig. 2.** *Cucumis* phylogenetic tree using the barcode of *ribulose-1,5-bisphosphate carboxylase/oxygenase large subunit* (*rbcl*).

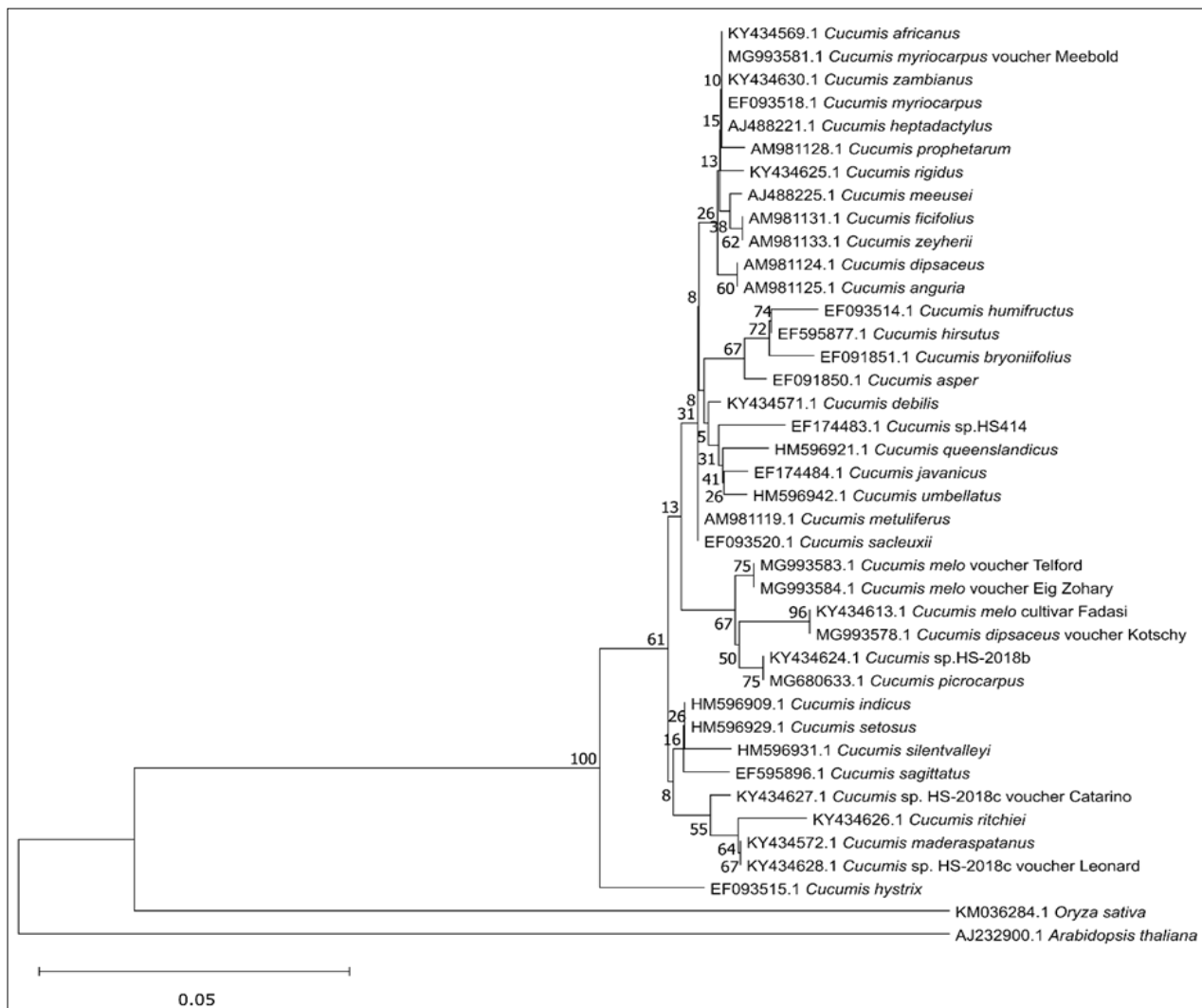


**Fig. 3.** *Cucumis* phylogenetic tree using the barcode of nrDNA (ITS1+5.8S+ITS2).

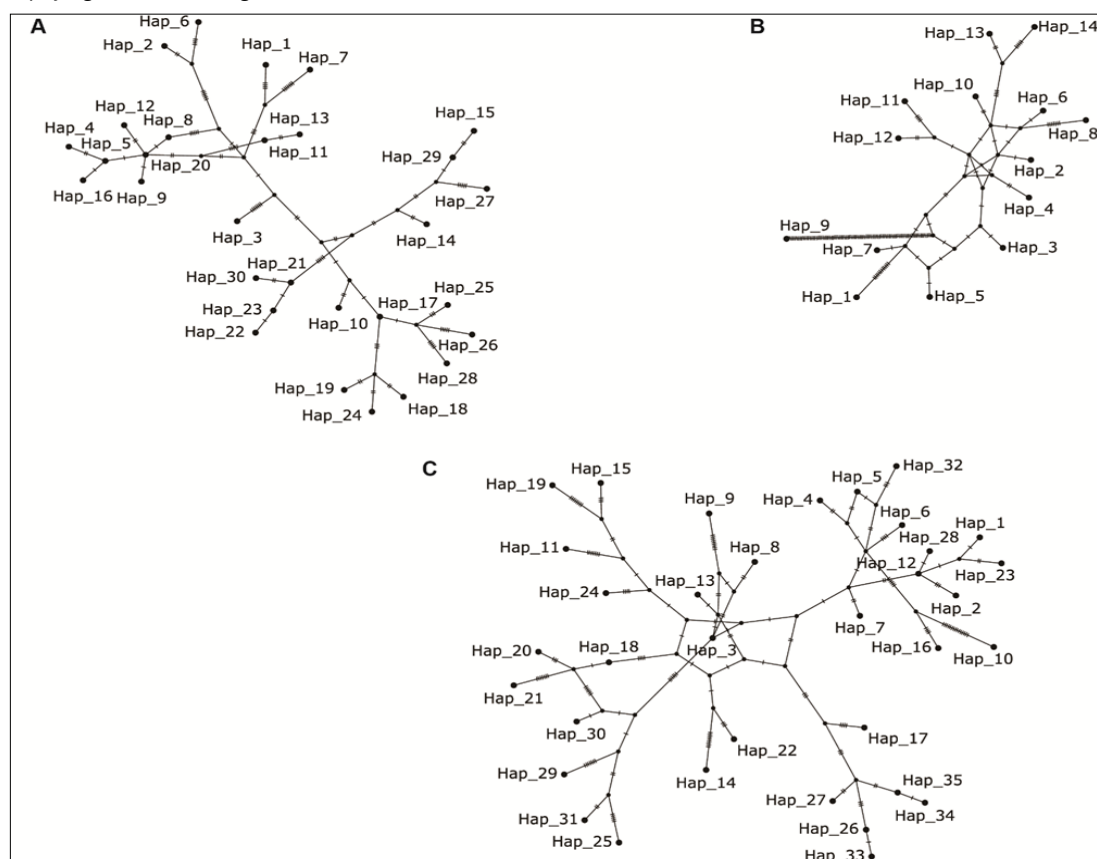


**Fig. 4.** Haplotype map of (A) *matK*, (B) *rbcL* and (C) *nrDNA* loci of *Cucumis* L. species. Hap = haplotype.

**Table 7.** Haplotype distribution of *Cucumis* and outgroup species using *matK*, *rbcl* and *nrDNA* loci

Hap	Distribution of <i>Cucumis</i> species based on loci		
	<i>matK</i>	<i>rbcl</i>	<i>nrDNA</i>
Hap_1	<i>C. bryoniifolius</i>	<i>C. anguria</i>	<i>C. heptadactylus</i>
Hap_2	<i>C. hirsutus</i>	<i>C. bryoniifolius</i>	<i>C. meeusei</i>
Hap_3	<i>C. sagittatus</i>	<i>C. hirsutus</i> , <i>C. heptadactylis</i> , <i>C. hystrix</i> , <i>C. prophetarum</i> , <i>C. indicus</i> , <i>C. meeusei</i> , <i>C. rigidus</i> , <i>C. dipsaceus</i>	<i>C. metuliferus</i>
Hap_4	<i>C. zeyherii</i>	<i>C. sagittatus</i>	<i>C. dipsaceus</i>
Hap_5	<i>C. heptadactylis</i> , <i>C. myriocarpus</i> , <i>C. anguria</i> , <i>C. myriocarpus</i> voucher Meebold	<i>C. zeyherii</i>	<i>C. anguria</i>
Hap_6	<i>C. humifructus</i>	<i>C. asper</i> , <i>C. saclexii</i> , <i>C. zambianus</i>	<i>C. prophetarum</i>
Hap_7	<i>C. asper</i>	<i>C. ficifolius</i> , <i>C. humifructus</i> , <i>C. myriocarpus</i> , <i>C. africanus</i> , <i>C. sp. HS-2018c</i> voucher Leonard, <i>C. maderaspatanus</i> , <i>C. ritchiei</i> , <i>C. setosus</i> , <i>C. silentvalleyi</i> , <i>C. myriocarpus</i> voucher Meebold	<i>C. ficifolius</i> , <i>C. zeyherii</i>
Hap_8	<i>C. dipsaceus</i>	<i>C. metuliferus</i>	<i>C. asper</i>
Hap_9	<i>C. ficifolius</i>	<i>C. javanicus</i>	<i>C. bryoniifolius</i>
Hap_10	<i>C. hystrix</i>	<i>C. sp. HS414</i> , <i>C. queenslandicus</i> , <i>C. umbellatus</i>	<i>C. humifructus</i>
Hap_11	<i>C. metuliferus</i>	<i>C. debilis</i>	<i>C. hystrix</i>
Hap_12	<i>C. prophetarum</i>	<i>C. sp. HS-2018c</i> voucher Catarino	<i>C. myriocarpus</i> , <i>C. myriocarpus</i> voucher Meebold
Hap_13	<i>C. saclexii</i>	<i>C. melo</i> cultivar Fadasi, <i>C. melo</i> voucher Eig Zohary, <i>C. melo</i> voucher Telford	<i>C. saclexii</i>
Hap_14	<i>C. javanicus</i>	<i>C. picrocarpus</i> , <i>C. sp. HS-2018b</i> , <i>C. dipsaceus</i> voucher Kotschy	<i>C. sp. HS414</i>
Hap_15	<i>C. sp. HS414</i>	ND	<i>C. javanicus</i>
Hap_16	<i>C. africanus</i>	ND	<i>C. hirsutus</i>
Hap_17	<i>C. debilis</i>	ND	<i>C. sagittatus</i>
Hap_18	<i>C. sp. HS-2018c</i> voucher Catarino	ND	<i>C. indicus</i>
Hap_19	<i>C. sp. HS-2018c</i> voucher Leonard, <i>C. maderaspatanus</i>	ND	<i>C. queenslandicus</i>
Hap_20	<i>C. meeusei</i> , <i>C. zambianus</i> , <i>C. rigidus</i>	ND	<i>C. setosus</i>
Hap_21	<i>C. melo</i> cultivar Fadasi, <i>C. melo</i> voucher Eig Zohary, <i>C. dipsaceus</i> voucher Kotschy	ND	<i>C. silentvalleyi</i>
Hap_22	<i>C. picrocarpus</i>	ND	<i>C. umbellatus</i>
Hap_23	<i>C. sp. HS-2018b</i>	ND	<i>C. africanus</i>
Hap_24	<i>C. ritchiei</i>	ND	<i>C. debilis</i>
Hap_25	<i>C. setosus</i>	ND	<i>C. maderaspatanus</i>
Hap_26	<i>C. silentvalleyi</i>	ND	<i>C. melo</i> cultivar Fadasi
Hap_27	<i>C. umbellatus</i>	ND	<i>C. sp. HS-2018b</i> , <i>C. picrocarpus</i>
Hap_28	<i>C. indicus</i>	ND	<i>C. rigidus</i>
Hap_29	<i>C. queenslandicus</i>	ND	<i>C. ritchiei</i>
Hap_30	<i>C. melo</i> voucher Telford	ND	<i>C. sp. HS-2018c</i> voucher Catarino
Hap_31	ND	ND	<i>C. sp. HS-2018c</i> voucher Leonard
Hap_32	ND	ND	<i>C. zambianus</i>
Hap_33	ND	ND	<i>C. dipsaceus</i> voucher Kotschy
Hap_34	ND	ND	<i>C. melo</i> voucher Telford
Hap_35	ND	ND	<i>C. melo</i> voucher Eig Zohary

Hap = haplotype, ND = not detected

## Conclusion

This study rigorously evaluated phylogenetic support values, genetic divergence and haplotype analyses to assess marker performance in *Cucumis* L. The analysis confirmed *nrDNA* as the most reliable marker, while plastid markers (*matK* and *rbcl*) showed lower resolution. The *nrDNA* provides the highest phylogenetic distinction, particularly among *Cucumis melo* accessions, whereas *matK* was moderately informative and *rbcl* had limited utility at the intraspecific level. To enhance the accuracy and robustness of future phylogenetic studies, an expansion of DNA barcode data for *Cucumis* species is essential to include a more comprehensive representation of the genus.

## Acknowledgements

The authors would like to thank the Laboratory of Plant Physiology and Breeding for providing the facilities. This

research has received funding support from the Faculty of Animal and Agricultural Sciences Universitas Diponegoro (grant number 10/UN7.F5/PP/II/2024).

## Authors' contributions

BH conceived the study and participated in its design and coordination, *in-silico* analysis and manuscript writing. FK conceived the study and participated in its design and coordination. MGAS conceived the study and participated in its design and coordination. AFI participated in writing the manuscript. SNA participated in the *in-silico* analysis. TBS participated in the *in-silico* analysis and wrote the manuscript. All authors read and approved the final manuscript.

## Compliance with ethical standards

**Conflict of interest:** Authors do not have any conflict of interest to declare.

**Ethical issues:** None

**Declaration of generative AI and AI-assisted technologies in the writing process:** During the preparation of this work, the authors used Grammarly to check grammar, spelling and style. After using this tool, the authors reviewed and edited the content as needed and takes full responsibility for the content of the publication.

## References

- Pichot C, Djari A, Tran J, Verdenaud M, Marande W, Huneau C et al. Cantaloupe melon genome reveals 3D chromatin features and structural relationship with the ancestral Cucurbitaceae karyotype. *iScience*. 2021; 25:103696. <https://doi.org/10.1016/j.isci.2021.103696>
- Christenhusz MJM, Byng JW. The number of known plant species in the world and its annual increase. *Phytotaxa*. 2016;261:201–17. <https://doi.org/10.11646/phytotaxa.261.3.1>
- Ghebretinsae AG, Thulin M, Barber JC. Relationships of cucumbers and melons unraveled: molecular phylogenetics of *Cucumis* and related genera (Benincaseae, Cucurbitaceae). *Am J Bot*. 2007;94(7):1256–66. <https://doi.org/10.3732/ajb.94.7.1256>
- Renner SS, Schaefer H, Kocyan A. Phylogenetics of *Cucumis* (Cucurbitaceae): Cucumber (*C. sativus*) belongs in an Asian/Australian clade far from melon (*C. melo*). *Evol Biol*. 2007;7:58. <https://doi.org/10.1186/1471-2148-7-58>
- Rolnik A, Olas B. Vegetables from the Cucurbitaceae family and their products: positive effect on human health. *Nutr*. 2020;78:110788. <https://doi.org/10.1016/j.nut.2020.110788>
- Martinez C, Jamilena M. To be a male or a female flower, a question of ethylene in cucurbits. *Curr Opin Plant Biol*. 2021;59:101981. <https://doi.org/10.1016/j.pbi.2020.101981>
- Grumet R, McCreight JD, McGregor C, Weng Y, Mazourek M, Reitsma K et al. Genetic resources and vulnerabilities of major Cucurbit crops. *Genes*. 2021;12:1222. <https://doi.org/10.3390/genes12081222>
- Yusuf AF, Wibowo WA, Subiastuti AS, Daryono BS. Morphological studies of stability and identity of melon (*Cucumis melo* L.) 'Hikapel' and comparative cultivars. In: AIP Conference Proceedings. 2020;2260(1). <https://doi.org/10.1063/5.0017606>
- Yusuf AF, Daryono BS. Studies of genetic and morphological characteristics of Indonesian melon (*Cucumis melo* L. 'Hikapel') germplasm. *Int J Adv Sci Eng Info Techno*. 2021;11:2023–30. <https://doi.org/10.18517/ijaseit.11.5.14047>
- Jin ZT, Hodel RGJ, Ma DK, Wang H, Liu GN, Ren C et al. Nightmare or delight: taxonomic circumscription meets reticulate evolution in the phylogenomic era. *Mol Phylogenet Evol*. 2023;189:107914. <https://doi.org/10.1016/j.ympev.2023.107914>
- Hinchliff CE, Smith SA, Allman JF, Cranston KA, Hillis DM. Synthesis of phylogeny and taxonomy into a comprehensive tree of life. *Proc Natl Acad Sci*. 2015;112:12764–69. <https://doi.org/10.1073/pnas.1423041111>
- Chung SM, Staub JE, Chen JF. Molecular phylogeny of *Cucumis* species as revealed by consensus chloroplast SSR marker length and sequence variation. *Genome*. 2006;49:219–29. <https://doi.org/10.1139/g05-101>
- Ling J, Xie X, Gu X, Zhao J, Ping X, Li Y et al. High-quality chromosome-level genomes of *Cucumis metuliferus* and *Cucumis melo* provide insight into *Cucumis* genome evolution. *Plant J*. 2021;107(1):136–48. <https://doi.org/10.1111/tpj.15279>
- Antil S, Abraham JS, Sripoorna S, Maurya S, Dagar J, Makhija S et al. DNA barcoding, an effective tool for species identification: A review. *Mol Biol Rep*. 2023;50:761–75. <https://doi.org/10.1007/s11033-022-08015-7>
- Letsiou S, Madesis P, Vasdekis E, Montemurro C, Grigoriou ME, Skavdis G et al. DNA barcoding as a plant identification method. *Appl Sci*. 2024;14(4):1415. <https://doi.org/10.3390/app14041415>
- Mathew D. DNA barcoding and its applications in horticultural crops. In: Lim CT, Goh JCH, editors. *Biotechnology in Horticulture: Methods and Applications*; India. Dordrecht: New India Publishing Agency; 2013. p. 25–50. <https://doi.org/10.5281/zenodo.836319>
- Kress WJ. Plant DNA barcodes: applications today and in the future. *J Syst Evol*. 2017;55:291–307. <https://doi.org/10.1111/jse.12254>
- Saidon NA, Wagiran A, Samad AFA, Mohd Salleh F, Mohamed F, Jani J et al. DNA barcoding, phylogenetic analysis and secondary structure predictions of *Nepenthes ampullaria*, *Nepenthes gracilis* and *Nepenthes rafflesiana*. *Genes*. 2023;14(3):697. <https://doi.org/10.3390/genes14030697>
- Linh NN, Trung LQ, Binh NQ, Ha LTT, Hang PLB, Hanh NP et al. DNA barcoding and phylogenetic analysis of the species in the genus *Alpinia*. *Int J Agric Biol*. 2023;29:227–34. <https://doi.org/10.17957/IJAB/15.2024>
- Prasetya E, Lazuardi F, Harahap F, Rachmawati Y, Yusuf Y, Al Idrus SI et al. Region of nuclear ribosomal DNA (*ITS2*) and chloroplast DNA (*rbcl* and *trnL-F*) as a suitable DNA barcode for identification of *Zingiber loerzingii* Valetton from North Sumatera, Indonesia. *J Trop Biodivers Biotech*. 2023;08:1–12. <https://doi.org/10.22146/jtbb.76956>
- Kiran KM, Sandeep BV. Phylogenetic study of mangrove associate grass *Myriostachya wightiana* (Nees ex Steud.) Hook. f. using *rbcl* gene sequence. *Plant Sci Today*. 2021;8:590–95. <https://doi.org/10.14719/pst.2021.8.3.1133>
- Ho VT, Tran TKP, Vu TTT, Ho VT, Widiarsih S. Comparison of *matK* and *rbcl* DNA barcodes for genetic classification of jewel orchid accessions in Vietnam. *J Genet Eng Biotechnol*. 2021;19(1):93. <https://doi.org/10.1186/s43141-021-00188-1>
- Duan H, Wang W, Zeng Y, Guo M, Zhou Y. The screening and identification of DNA barcode sequences for *Rehmannia*. *Sci Rep*. 2019;9:17295. <https://doi.org/10.1038/s41598-019-53752-8>
- Kang Y, Deng Z, Zang R, Long W. DNA barcoding analysis and phylogenetic relationships of tree species in tropical cloud forests. *Sci Rep*. 2017;7:12564. <https://doi.org/10.1038/s41598-017-13057-0>
- Talavera G, Lukhtanov V, Pierce NE, Vila R. DNA barcodes combined with multilocus data of representative taxa can generate reliable higher-level phylogenies. *Syst Biol*. 2022;71:382–95. <https://doi.org/10.1093/sysbio/syab038>
- Retnaningati D. Intraspecific phylogenetic relationship of *Cucumis melo* L. based on DNA barcode gen *matK*. *Biota*. 2017;2:62–67. <https://doi.org/10.24002/biota.v2i2.1658>
- Ho VT, Nguyen MP. An *in silico* approach for evaluation of *rbcl* and *matK* loci for DNA barcoding of Cucurbitaceae family. *Biodiversitas*. 2020;21:3879–3885. <https://doi.org/10.13057/biodiv/d210858>
- Sholiha FU, Yuniastuti E, Hartati S. The *matK* gene analysis in five types of matoa (*Pometia pinnata* J.R. Forst. & G. Forst) based on the pericarp colour. *J Appl Biol Biotechnol*. 2024;12(3):54–58. <https://doi.org/10.7324/JABB.2024.167495>
- Wu CT, Hsieh CC, Lin WC, Tang CY, Yang CH, Huang YC, Ko YJ. Internal transcribed spacer sequence-based identification and phylogenetic relationship of I-Tiao-Gung originating from *Flemingia* and *Glycine* (Leguminosae) in Taiwan. *J Food Drug Anal*. 2013;21(4):356–62. <https://doi.org/10.1016/j.jfda.2013.08.002>
- Omonhinmin CA, Olomukoro EE, Onuselogu CC, Popoola JO, Oyejide SO. Intra-specific genetic variability dataset on *rbcl* gene



- in *Moringa oleifera* Lam. (Moringaceae) in Nigeria. Data in Brief. 2023;50:109399. <https://doi.org/10.1016/j.dib.2023.109399>
31. Li Q, Li H, Huang Wu, Xu Y, Zhou Q, Wang S, Ruan J, Huang S, Zhang Z. A chromosome-scale genome assembly of cucumber (*Cucumis sativus* L.). GigaScience. 2019;8(6):giz072. <https://doi.org/10.1093/gigascience/giz072>
  32. Johnson MS, Venkataram S, Kryazhimskiy S. Best practices in designing, sequencing and identifying random DNA barcodes. J Mol Evol. 2023;91:263–80. <https://doi.org/10.1007/s00239-022-10083-z>
  33. Qin X, Zhang Z, Lou Q, Xia L, Li J, Li M, et al. Chromosome-scale genome assembly of *Cucumis hystrix*– A wild species interspecifically cross-compatible with cultivated cucumber. Hortic Res. 2021;8:40. <https://doi.org/10.1038/s41438-021-00475-5>
  34. Hu J, Yao J, Lu J, Liu W, Zhao Z, Li Y, et al. The complete chloroplast genome sequences of nine melon varieties (*Cucumis melo* L.): lights into comparative analysis and phylogenetic relationships. Front Genet. 2024;15:1417266. <https://doi.org/10.3389/fgene.2024.1417266>
  35. Pere K, Mburu K, Muge EK, Wagacha JM, Nyaboga EN. Molecular discrimination and phylogenetic relationships of *Physalis* species based on *ITS2* and *rbcl* DNA barcode sequence. Crops. 2023;3:302–19. <https://doi.org/10.3390/crops3040027>
  36. Carlin JL. Mutations are the raw materials of evolution. Nature Education Knowledge. 2011;3:10.
  37. Mendez-Harclerode FM, Strauss RE, Fulhorst CF, Milazzo ML, Ruthven DC, Bradley RD. Molecular evidence for high levels of intrapopulation genetic diversity in woodrats (*Neotoma micropus*). J Mammal. 2007;88:360–70. <https://doi.org/10.1644/05-MAMM-A-377R1.1>
  38. Tamura K, Peterson D, Peterson N, Stecher G, Nei M, Kumar S. MEGA5: molecular evolutionary genetics analysis using maximum likelihood, evolutionary distance and maximum parsimony methods. Mol Biol and Evol. 2011;28(10):2731–39. <https://doi.org/10.1093/molbev/msr121>
  39. Liu H, Ye H, Wang J, Chen S, Li M, Wang G, et al. Genome-wide identification and characterization of YABBY gene family in *Juglans regia* and *Juglans mandshurica*. Agron. 2022;12:1914. <https://doi.org/10.3390/agronomy12081914>
  40. Wang J, Yuan M, Feng Y, Zhang Y, Bao S, Hao Y, et al. A common whole-genome paleotetraploidization in Cucurbitales. Plant Physiol. 2022;190(4):2430–48. <https://doi.org/10.1093/plphys/kiac410>
  41. Endl J, Achigan-Dako EG, Pandey AK, Monforte AJ, Pico B, Schaefer H. Repeated domestication of melon (*Cucumis melo*) in Africa and Asia and a new close relative from India. Am J Bot. 2018;105(10):1662–71. <https://doi.org/10.1002/ajb2.1172>
  42. Sebastian P, Schaefer H, Telford IRH, Renner SS. Cucumber (*Cucumis sativus*) and melon (*C. melo*) have numerous wild relatives in Asia and Australia and the sister species of melon is from Australia. Proc Natl Acad Sci USA. 2010;107(32):14269–73. <https://doi.org/10.1073/pnas.1005338107>
  43. Ramesh GA, Mathew D, John KJ, Ravisankar V. Chloroplast gene *matK* holds the barcodes for identification of *Momordica* (Cucurbitaceae) species from Indian subcontinent. Hortic Plant J 2022;8:89–98. <https://doi.org/10.1016/j.hpj.2021.04.001>
  44. Tabita FR, Hanson TE, Satagopan S, Witte BH, Kreel NE. Phylogenetic and evolutionary relationships of RubisCO and the RubisCO-like proteins and the functional lessons provided by diverse molecular forms. Philos Trans R Soc B: Biol Sci. 2008;363 (1504):2629–40. <https://doi.org/10.1098/rstb.2008.0023>
  45. Reddy BU. Cladistic analyses of a few members of Cucurbitaceae using *rbcl* nucleotide and amino acid sequences. Int J Bioinform Res. 2009;1:58–64. <https://doi.org/10.9735/0975-3087.1.2.58-64>
  46. Yong WTL, Mustafa AA, Derise MR, Rodrigues KF. DNA barcoding using chloroplast *matK* and *rbcl* regions for the identification of bamboo species in Sabah. Adv Bamboo Sci. 2024;7:100073. <https://doi.org/10.1016/j.bamboo.2024.100073>
  47. Liu ZF, Ma H, Zhang XY, Ci XQ, Li L, Hu JL, et al. Do taxon-specific DNA barcodes improve species discrimination relative to universal barcodes in Lauraceae? Bot J Linn Soc. 2022;199:741–53. <https://doi.org/10.1093/botlinnean/boab089>
  48. Almontero CC, Lalusin AG, Diaz MGQ, Ocampo ETM, Gentallan RP Jr, Rojas SM. DNA barcoding of 11 endemic *Vanda* species of the Philippines based on *rbcl*, *matK* and *ITS* sequences. Philipp J Sci. 2024;153(5):1783–800.
  49. He S, Xu B, Chen S, Li G, Zhang J, Xu J, et al. Sequence characteristics, genetic diversity and phylogenetic analysis of the *Cucurbita ficifolia* (Cucurbitaceae) chloroplasts genome. Genom. 2024;25:384. <https://doi.org/10.1186/s12864-024-10278-2>

#### Additional information

**Peer review:** Publisher thanks Sectional Editor and the other anonymous reviewers for their contribution to the peer review of this work.

**Reprints & permissions information** is available at [https://horizonpublishing.com/journals/index.php/PST/open\\_access\\_policy](https://horizonpublishing.com/journals/index.php/PST/open_access_policy)

**Publisher's Note:** Horizon e-Publishing Group remains neutral with regard to jurisdictional claims in published maps and institutional affiliations.

**Indexing:** Plant Science Today, published by Horizon e-Publishing Group, is covered by Scopus, Web of Science, BIOSIS Previews, Clarivate Analytics, NAAS, UGC Care, etc  
See [https://horizonpublishing.com/journals/index.php/PST/indexing\\_abstracting](https://horizonpublishing.com/journals/index.php/PST/indexing_abstracting)

**Copyright:** © The Author(s). This is an open-access article distributed under the terms of the Creative Commons Attribution License, which permits unrestricted use, distribution and reproduction in any medium, provided the original author and source are credited (<https://creativecommons.org/licenses/by/4.0/>)

**Publisher information:** Plant Science Today is published by HORIZON e-Publishing Group with support from Empirion Publishers Private Limited, Thiruvananthapuram, India.